

1 **Significant role of biomass burning in heavy haze**
2 **formation in a megacity: Molecular-level insights from**
3 **intensive PM_{2.5} sampling on winter hazy days**

4 Mingjie Kang^{1,2}, Mengying Bao^{1,2,3}, Wenhui Song^{1,2}, Aduburexiati Abulimiti^{1,2}, Fang
5 Cao^{1,2}, Sönke Szidat⁴, Yanlin Zhang^{1,2}

6 ¹ School of Ecology and Applied Meteorology, Nanjing University of Information Science and
7 Technology. Nanjing 210044, China.

8 ² Atmospheric Environment Center, Joint Laboratory for International Cooperation on Climate and
9 Environmental Change, Ministry of Education, Nanjing University of Information Science and
10 Technology. Nanjing 210044, China.

11 ³ Huzhou Meteorological Administration, Huzhou, 313000, China

12 ⁴ Department of Chemistry, Biochemistry and Pharmaceutical Sciences & Oeschger Centre for Climate
13 Change Research, University of Bern, Bern, 3012, Switzerland

14
15 Correspondence to: Yanlin Zhang (zhangyanlin@nuist.edu.cn; dryanlinzhang@outlook.com)

16
17

18 **Text S1: The isomeric ratios of anhydrosugars**

19 The isomeric ratios of anhydrosugars are good indicators of biofuels. For instance, the ratio of
20 levoglucosan to mannosan (L/M) tends to be higher for hardwood and crop residues than those
21 for softwood (Engling et al., 2006; Sang et al., 2013; Schmidl et al., 2008; Zhu et al., 2015).
22 Additionally, smoke particles emitted from crop straws, grasses, and biomass briquettes
23 combustion were reported to contain higher amounts of galactosan than mannosan (Fu et al.,
24 2008; Oros et al., 2006; Sheesley et al., 2003). Therefore, the lower L/M and M/G ratios during
25 the first episode ($\text{PM}_{2.5} > 200 \mu\text{g m}^{-3}$) likely indicate mixed contributions from softwood and
26 crop burning to heavy haze formation (Figure S9). In fact, the impact of softwood combustion
27 becomes larger in winter according to the previous report by Cheng (2013). However, the
28 contribution of hardwood burning could not be neglected either, especially in moderate haze
29 events (Figure S8a and Figure S9). This is supported by the rising L/M values with decreasing
30 $\text{PM}_{2.5}$ levels as shown in Figure S8b.

31 **Text S2: Chloride in $\text{PM}_{2.5}$ samples**

32 Chlorine plays a part in global tropospheric chemistry, affecting the atmospheric
33 oxidation capacity and consequently affecting the formation of $\text{PM}_{2.5}$ and O_3 ,
34 particularly in winter (Wang et al., 2019, 2020; Yi et al., 2023). In this study, the
35 absolute abundance of particulate Cl^- decreased with falling $\text{PM}_{2.5}$ levels (1.88-10.2 μg
36 m^{-3}), while its relative contributions to total $\text{PM}_{2.5}$ were on the rise (from 3.2% to 8.7%)
37 (Figure 4). An early study concluded that low temperature and high RH facilitate the
38 generation of $\text{PM}_{2.5}$ -bound Cl^- (Wang et al., 2023), which can account for high Cl^-
39 concentrations in first episode. Based on the backward trajectories of air masses in
40 Figure S1 and S2, roughly three sorts of trajectories were found in Nanjing during the
41 whole sampling period, i.e., continental, marine, and mixed airmasses. Marine sources
42 dominate the global tropospheric chlorine budget mainly through mobilization of
43 chloride from sea-salt aerosols (Wang et al., 2019), as indicated by the obvious
44 correlation between Cl^- and Na^+ ($r = 0.64$, $p < 0.01$). The rising Cl^- proportion with
45 decreasing $\text{PM}_{2.5}$ level might be linked to growing influences of sea-salt aerosols via
46 long-range atmospheric transport. In China, however, chlorine is mostly anthropogenic,

47 including coal combustion, BB, waste incineration, and industrial processes (Fu et al.,
48 2018; Li et al., 2012; Yang et al., 2018). The positive relationship of Cl^- with
49 levoglucosan proves a possible source of BB over this site ($r = 0.50$, $p < 0.05$). The
50 higher mass ratios of Cl^-/Na^+ (about 5.5-15.5) in these samples than sea water (1.81)
51 also indicate a significant contribution of anthropogenic sources to Cl^- in wintertime
52 haze over Nanjing. The concentrations of Cl^- measured in this study (average: $6.38 \pm$
53 $2.00 \mu\text{g m}^{-3}$) are comparable to those observed in winter in Beijing (Wang et al., 2005)
54 but slightly higher than those in a coastal megacity of Shanghai, China (Wang et al.,
55 2006; Ye et al., 2003).

56 **Text S3: Unsaturated diacids**

57 Maleic (cis-isomer) and fumaric (trans-isomer) acid are two principal aliphatic unsaturated
58 diacids found in this study, with concentration ranges of 0.86-41.9 ng m^{-3} and 1.61-27.6 ng m^{-3} ,
59 respectively. Significant correlation between fumaric and maleic acid ($r = 0.81$, $p < 0.01$)
60 suggests they may share common sources. In fact, maleic acid, which is a probable product
61 from photochemical oxidation of benzene, could be isomerized photochemically to trans
62 configuration (fumaric acid) in the air with solar radiation, thus M/F ratios depend on the
63 production of maleic acid and the subsequent transformation to fumaric acid. The M/F ratios
64 were higher in second episode with high temperature and low RH (average: 1.38 ± 0.35), but
65 lower in other two episodes (average: 0.71 ± 0.28 and 0.85 ± 0.44 , respectively). Higher M/F
66 values may be attributed to the superior photochemical generation of maleic acid over the cis-
67 to-trans isomerization at high ambient temperature and low RH, whereas lower ratios might be
68 in part due to the depressed maleic acid production by low temperature (Kawamura and
69 Ikushima, 1993).

70 **Text S4: Monocarboxylic acids**

71 Two monocarboxylic acids, formic and acetic acid, were determined too. Both formic and acetic
72 acids showed a decreasing temporal trend with decreasing $\text{PM}_{2.5}$ values, with the highest
73 concentrations appearing in the heaviest haze events (average: $0.18 \pm 0.05 \mu\text{g m}^{-3}$ for formic
74 acid and $0.22 \pm 0.11 \mu\text{g m}^{-3}$ for acetic acid, respectively). Lower temperature and higher RH in

75 this episode favor gas to particle conversion leading to high particulate concentrations. A clear
76 relationship between formic and acetic acid existed ($r = 0.88$, $p < 0.01$), suggesting similar
77 sources. Furthermore, formic and acetic acid both correlated significantly with levoglucosan (r
78 $= 0.73$, $p < 0.01$ and $r = 0.61$, $p < 0.01$, respectively), indicating BB is a significant source of
79 these acids. Formic acid was associated with EC as well ($r = 0.67$, $p < 0.01$), demonstrating
80 fossil fuel is another contributor. Actually, secondary sources are also important in the
81 atmospheric budgets of formic and acetic acids (Paulot et al., 2011). The ratio of acetic to formic
82 acid (A/F) can be used to estimate relative importance of primary emissions (> 1) and secondary
83 photochemical transformations (< 1) to carboxylic acids (Wang et al., 2007). The average A/F
84 ratio for three episodes was 1.15 ± 0.32 , 1.30 ± 0.52 , 1.1 ± 0.30 , respectively, suggesting
85 relatively larger contributions from primary sources, such as BB, vegetation, coal burning,
86 vehicular exhausts, and soil emissions in heating season (Khare et al., 1999; Stavrakou et al.,
87 2012; Wang et al., 2007).

88 **Text S5: Other identified chemicals**

89 Methylglyoxal (MeGly) was also detected in these $PM_{2.5}$ aerosols, which are oxidation products
90 from biogenic (e.g., isoprene/monoterpenes) and anthropogenic precursors (e.g., benzene,
91 toluene, and xylenes) (Kampf et al., 2012). Most carbonyls are present in gas phase in the
92 atmosphere. Thus, the high levels of MeGly observed in highest- $PM_{2.5}$ episode (20.4 ± 29.2 ng
93 m^{-3}) might be due to lower temperature that allows more gaseous carbonyls partitioning into
94 aerosol phase (Meng et al., 2018). In addition, fresh plumes from high BB activities during that
95 time may play a role as well (Kampf et al., 2012). The MeGly abundances in other two episodes
96 (10.1 ± 4.93 ng m^{-3} and 6.43 ± 3.04 ng m^{-3} , respectively) were comparable to those from Beijing
97 $PM_{2.5}$ samples (average: 8.3 ± 7.9 ng m^{-3}) (Zhao et al., 2018). A significant correlation between
98 MeGly and ^{14}C -WSOC was obtained in this study ($r = 0.74$, $p < 0.01$), suggesting non-fossil
99 sources such as BB may contribute to atmospheric MeGly.

100 Methanesulfonic acid (MSA) is an oxidation product of dimethylsulfide (DMS) mainly released
101 by marine phytoplankton. Thus MSA has long been regarded as a useful tracer for marine
102 biogenic sulfur production (Chen et al., 2012; Legrand and Pasteur, 1998). Surprisingly,
103 relatively abundant MSA was detected in this study, with higher levels occurring in the most

104 polluted episode ($0.09 \pm 0.02 \mu\text{g m}^{-3}$) compared with other two episodes ($0.04 \pm 0.01 \mu\text{g m}^{-3}$
105 and $0.02 \pm 0.01 \mu\text{g m}^{-3}$, respectively). These values are similar to those reported from $\text{PM}_{2.5}$
106 aerosol in Beijing (Wang et al., 2005). Yuan et al. (2004) pointed out that anthropogenic sources,
107 such as industrial emissions, could be additional sources for MSA in urban atmosphere. The
108 ratio of $\text{MSA}/\text{nss-SO}_4^{2-}$ (non-sea-salt sulfate) can be used to evaluate the relative contribution
109 of marine sulfur emissions to total sulfur budget in the atmosphere (Legrand and Pasteur, 1998).
110 On average, $\text{MSA}/\text{nss-SO}_4^{2-}$ ratios for three episodes are 0.003 ± 0.001 , 0.002 ± 0.00 , $0.002 \pm$
111 0.001 , respectively. Such low values indicate the influences of marine biogenic sources from
112 coastal and oceanic areas on urban haze formation are rather weak. The significant relationships
113 between MSA and levoglucosan ($r = 0.75$, $p < 0.01$) imply BB could be an important source of
114 MSA in addition to industrial emissions, which is also supported by the significant relationship
115 of non-fossil WSOC with MSA ($r = 0.79$, $p < 0.01$).

116

117

118
119
120
121
122
123
124
125
126
127
128
129
130
131
132
133
134
135
136
137
138
139
140
141
142
143
144
145
146
147
148
149
150
151
152
153
154
155
156
157
158
159
160
161

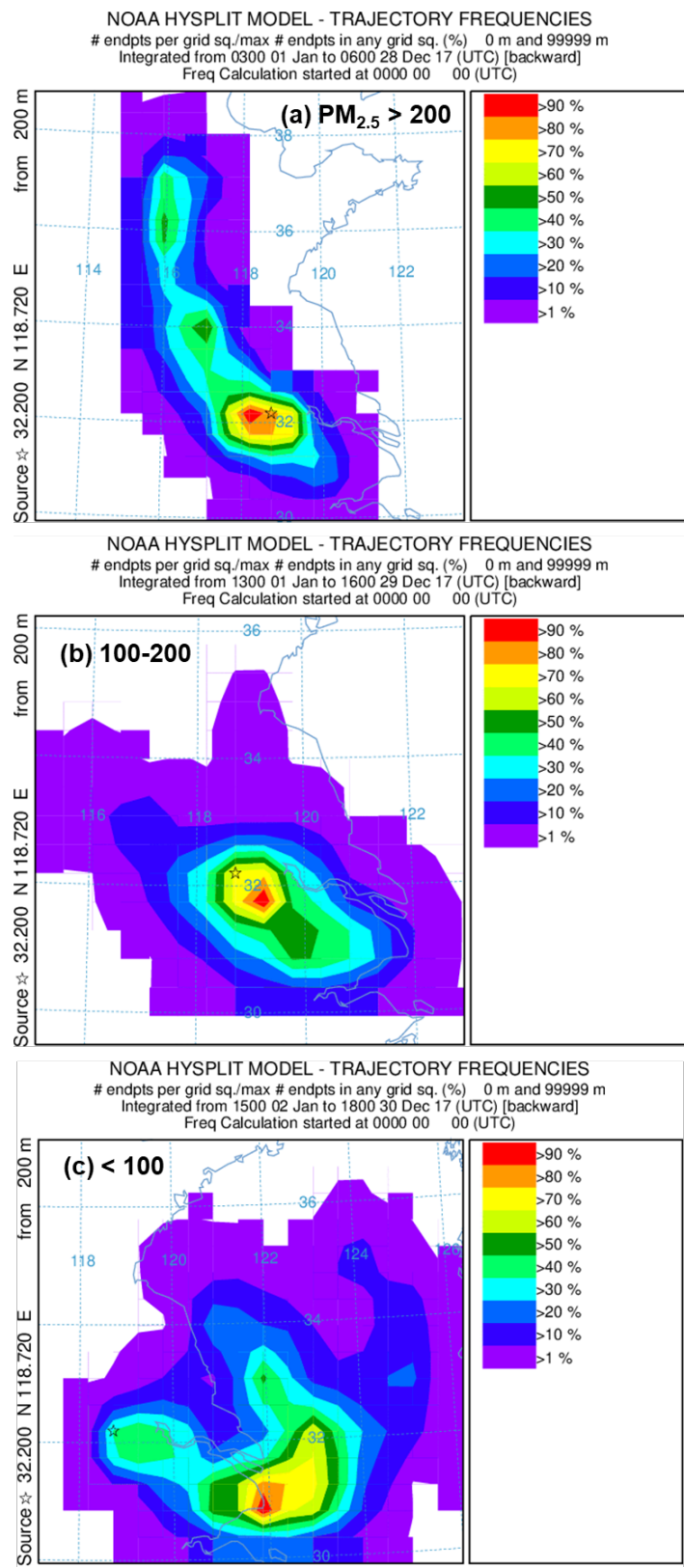
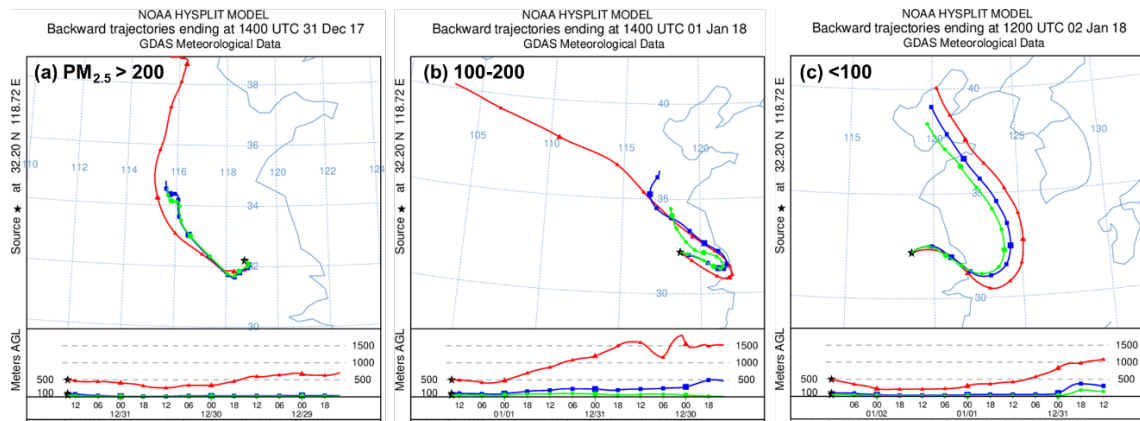


Figure S1. HYSPLIT back trajectories initiated over Nanjing with the altitude of these trajectories remaining below 200 m in the 48 h of the runs in three episodes according to $PM_{2.5}$ concentrations. The black star indicates the sampling site.

162

163



164

165

166

167

168

169

170

171

172

173

Figure S2. Three-day HYSPLIT back trajectories initiated over Nanjing with the altitude of these trajectories remaining below 500 m in the 72 h of the runs on the more polluted days in three episodes according to PM_{2.5} concentrations. The black star indicates the sampling site.

174
175
176
177
178
179
180
181
182
183
184
185
186
187
188
189
190
191
192
193
194
195
196
197
198
199
200
201
202
203
204
205
206
207
208
209
210
211
212

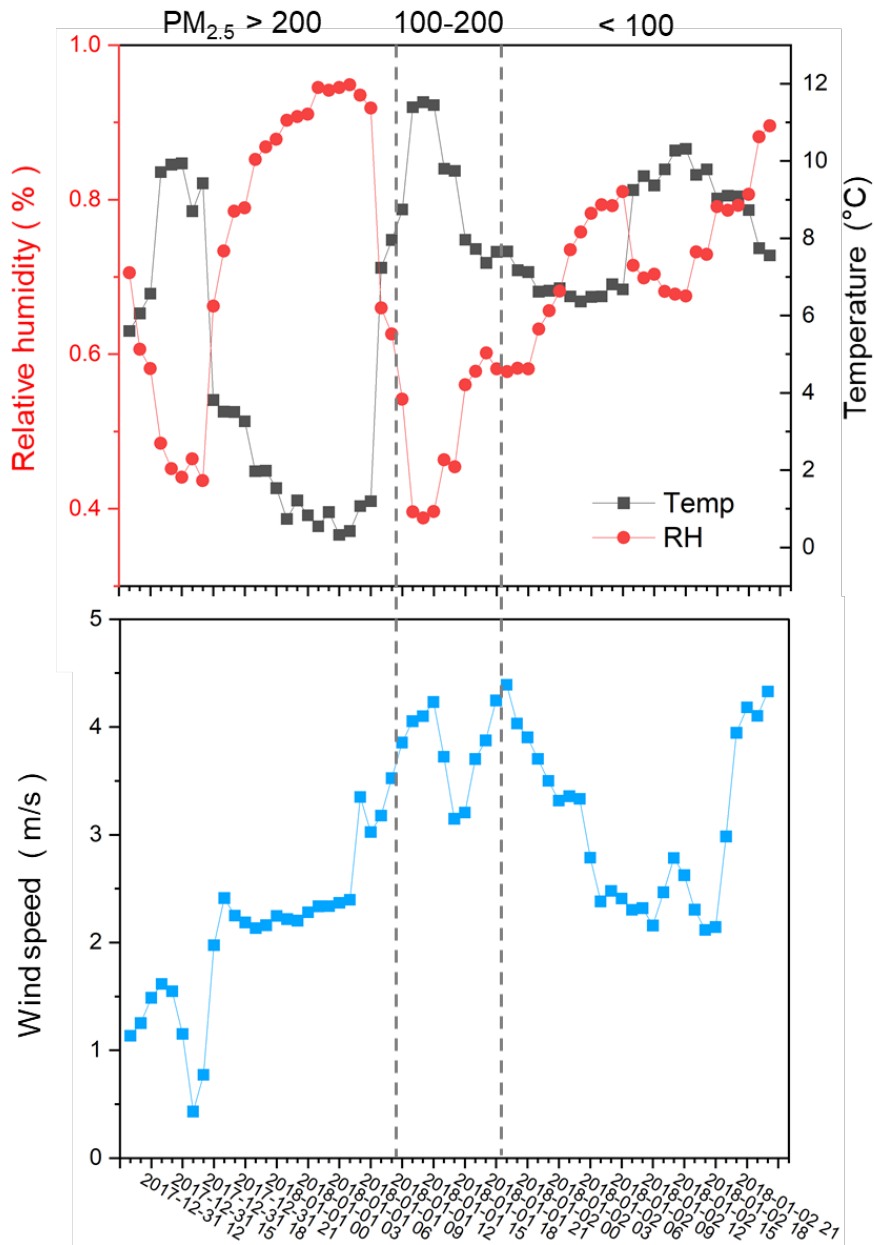


Figure S3. Time series of meteorological parameters (i.e., relative humidity, temperature, and wind speed) during sampling period in urban Nanjing.

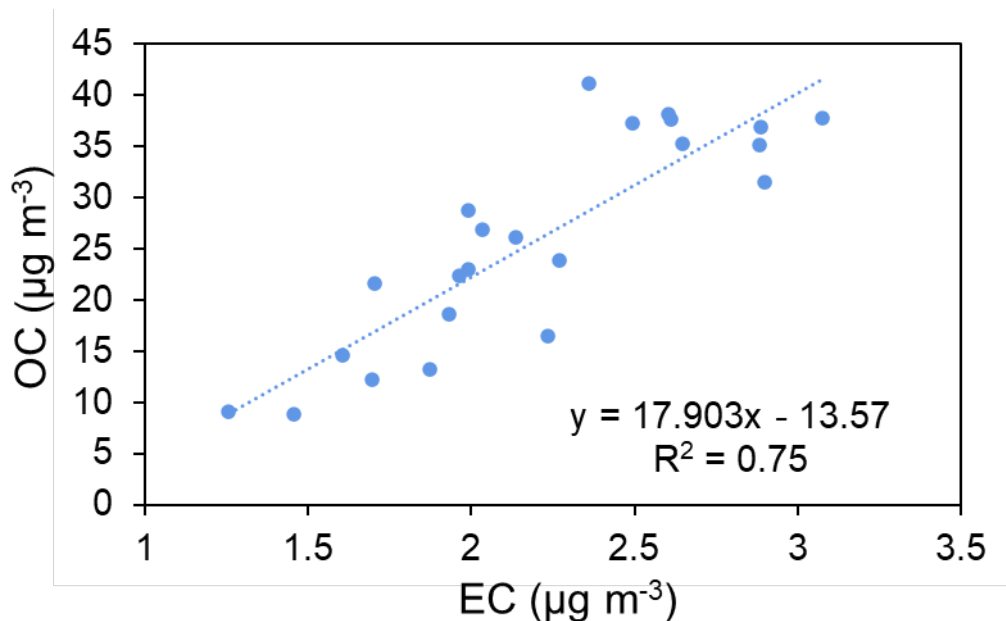
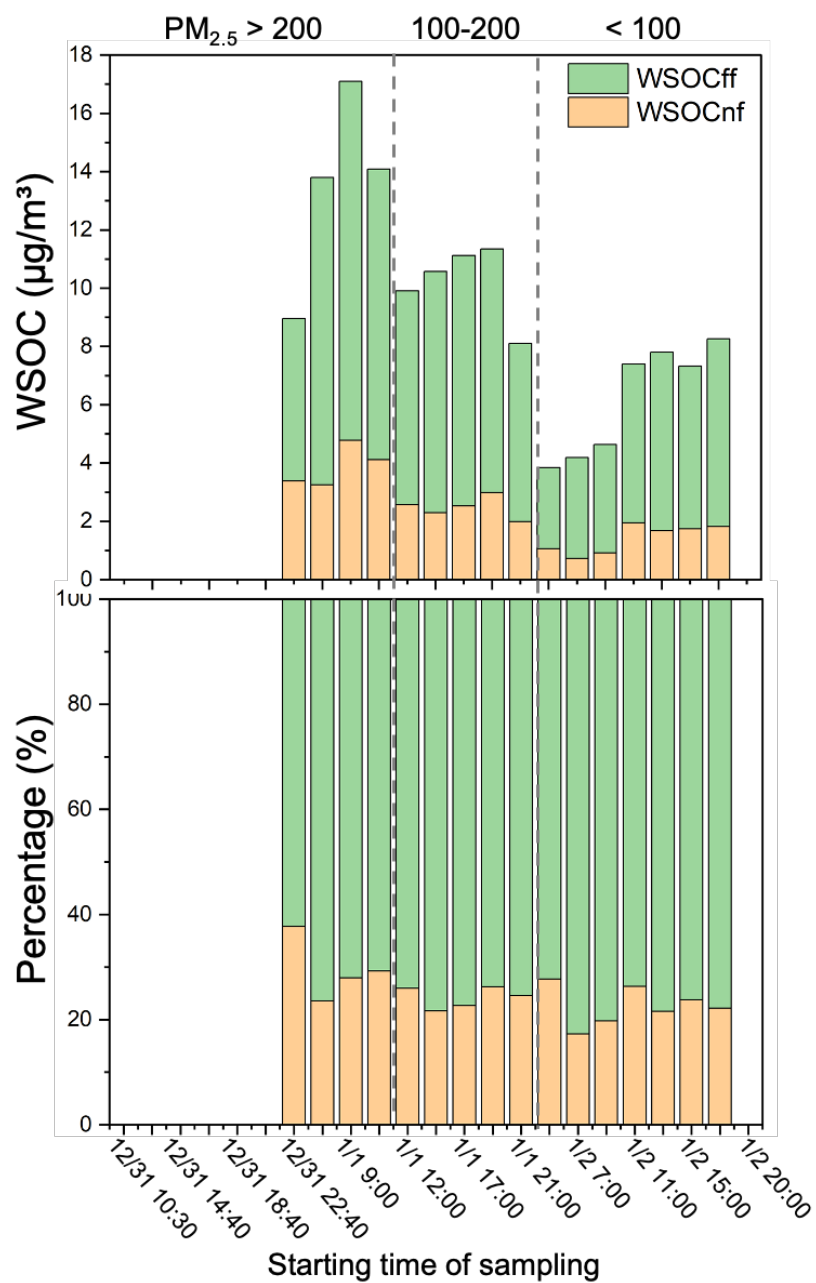


Figure S4. Based on the higher abundances of MSA and diacids in MBA together with nss-SO_4^{2-} (0.3 to $10.4 \mu\text{g m}^{-3}$), we suggest that these water-soluble organics as well as nss-SO_4^{2-} might enhance the hygroscopic growth of the ambient aerosols over the open ocean waters characterized by high biological activity, acting as CCN. GRL High abundances of oxalic, azelaic, and glyoxylic acids and methylglyoxal in the open ocean with high biological activity: Implication for secondary OA formation from isoprene



237

238 **Figure S5.** Temporal variations of fossil (ff) and non-fossil (nf) contribution to water-
 239 soluble organic carbon (WSOC) in 2-hour PM_{2.5} samples in Nanjing.

240

241
 242
 243
 244
 245
 246
 247
 248
 249
 250
 251
 252
 253
 254
 255
 256
 257
 258
 259
 260
 261
 262
 263
 264
 265
 266
 267

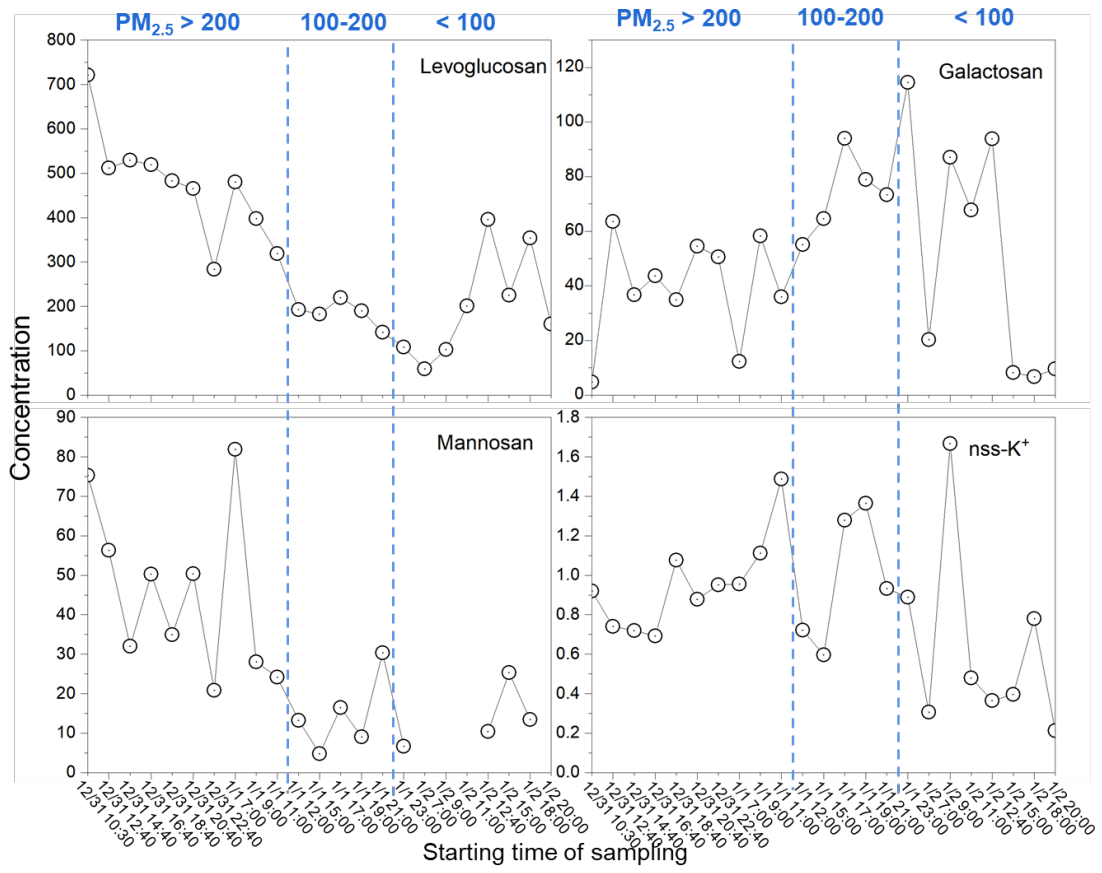
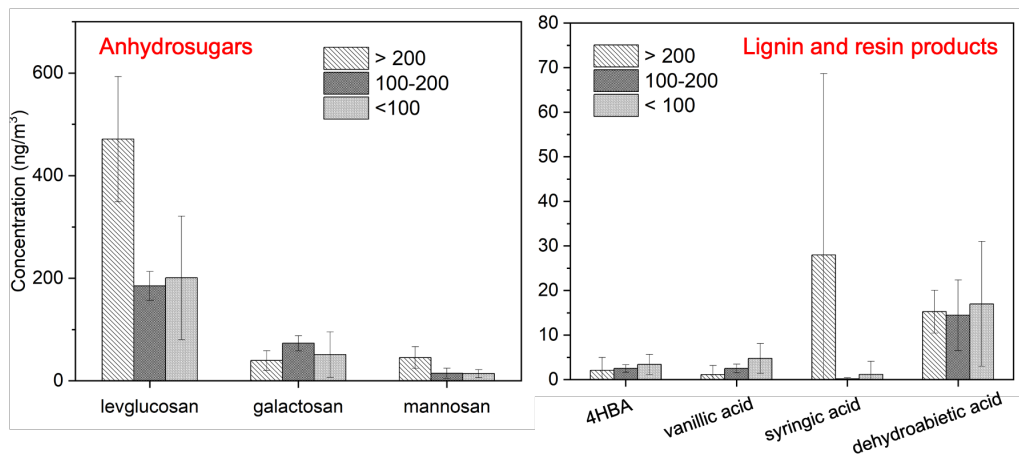
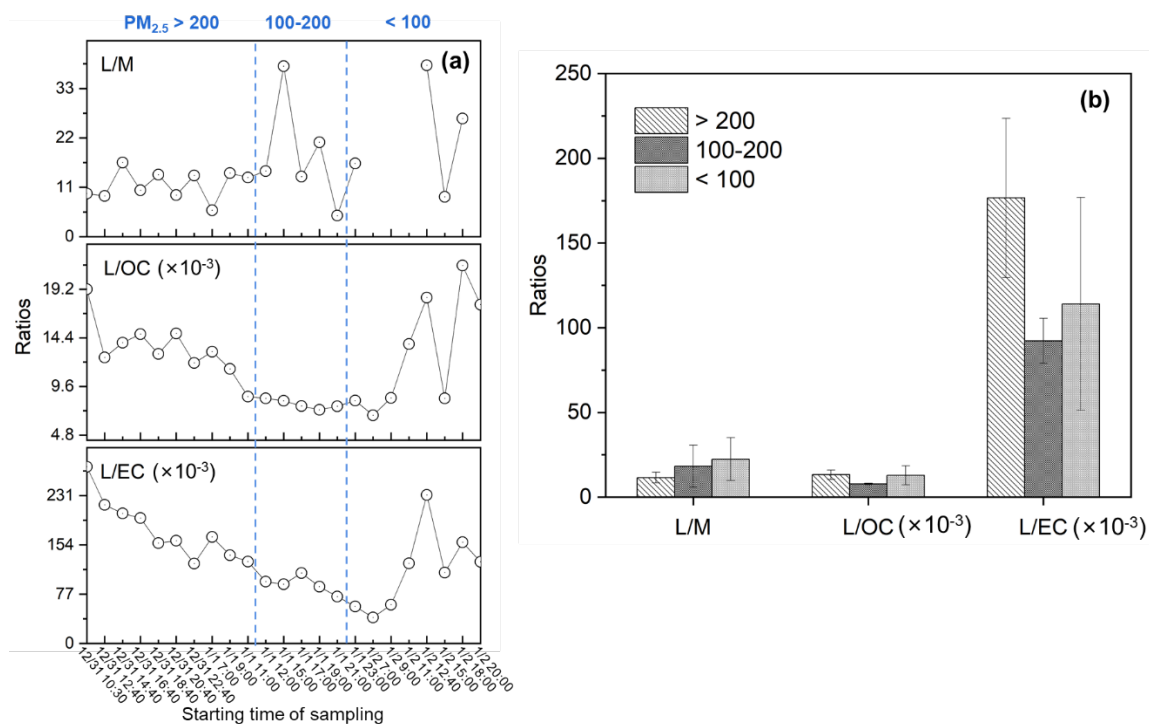


Figure S6. Temporal variations of biomass burning tracers including anhydrosugars (levoglucosan, galactosan, and mannosan, ng m⁻³) and non-sea-salt K⁺ (µg m⁻³).



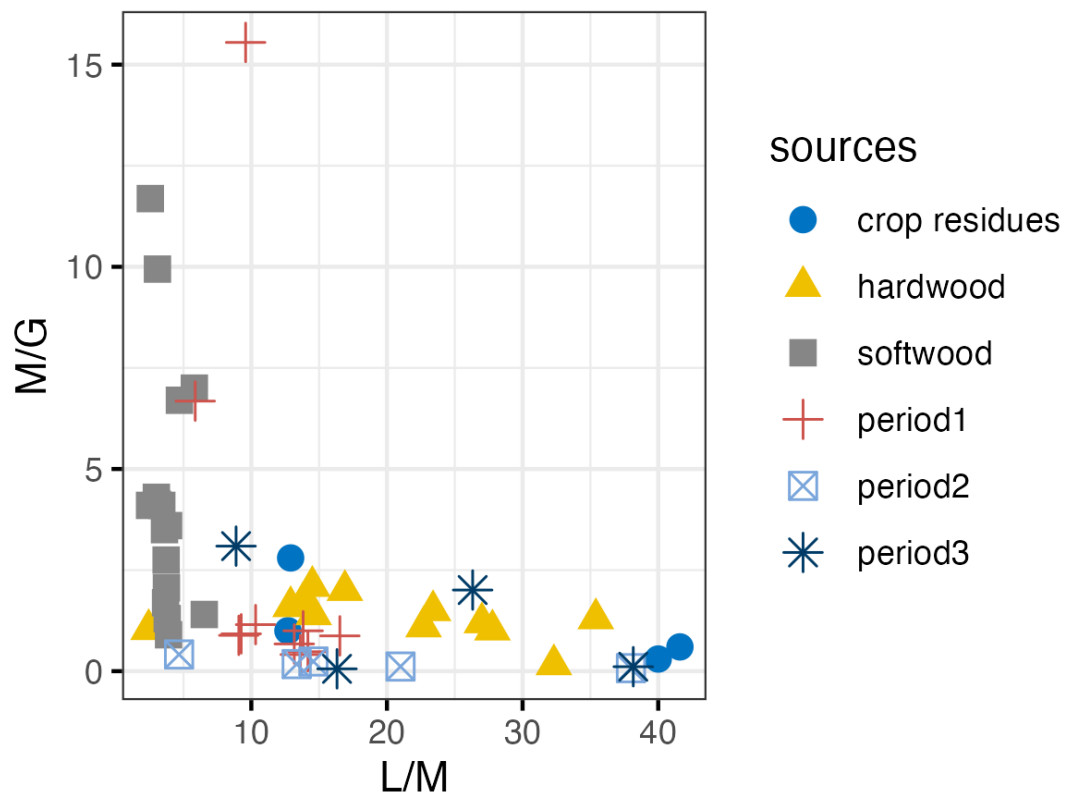
268
 269
 270
 271
 272
 273
 274
 275

Figure S7. Average concentrations of measured biomass burning tracers during three episodes with $PM_{2.5}$ levels in the ranges of > 200 , $100-200$, and $< 100 \mu g m^{-3}$, respectively.



276
 277
 278
 279
 280
 281
 282
 283

Figure S8. (a) Temporal variations of ratios of L/M, L/OC, and L/EC, and (b) the average ratios during three episodes (> 200 , $100-200$, and $< 100 \mu g m^{-3}$). L refers to levoglucosan, M is mannosan, OC means organic carbon, EC is elemental carbon.



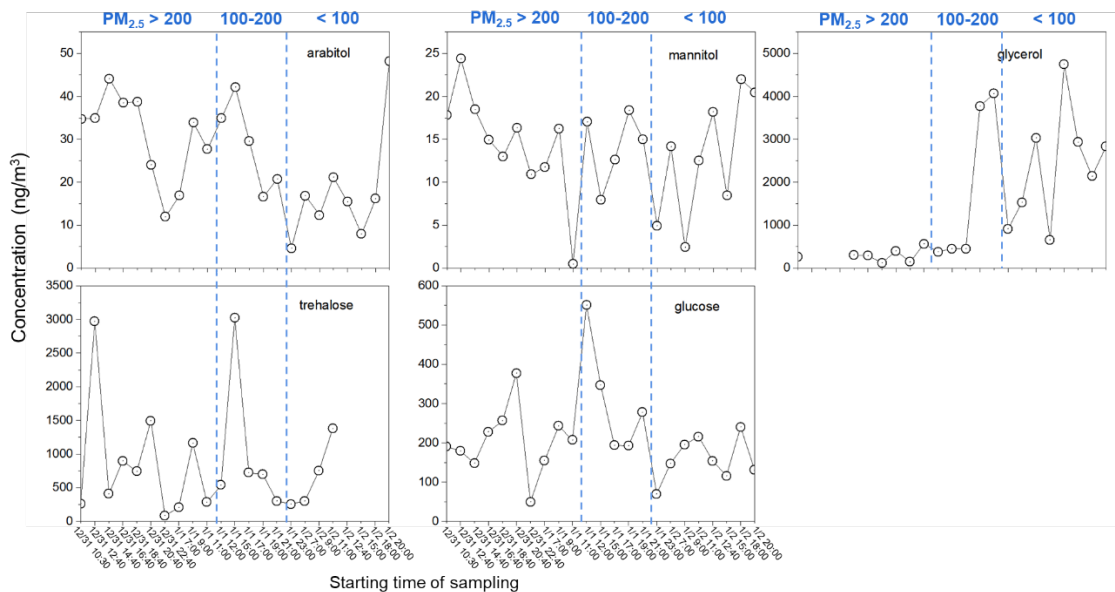
285

286 **Figure S9.** Comparison of L/M and M/G ratios from source emissions (literature values)
 287 and ambient aerosols in this study. L/M=levoglucosan to mannosan; M/G=mannosan
 288 to galactosan.

289

290

291



293

294 **Figure S10.** Temporal variations of sugars and sugar alcohols (ng/m³).

295

296

297

298

299

300

301

302

303

304

305

306

307

308

309

310

311

312

313

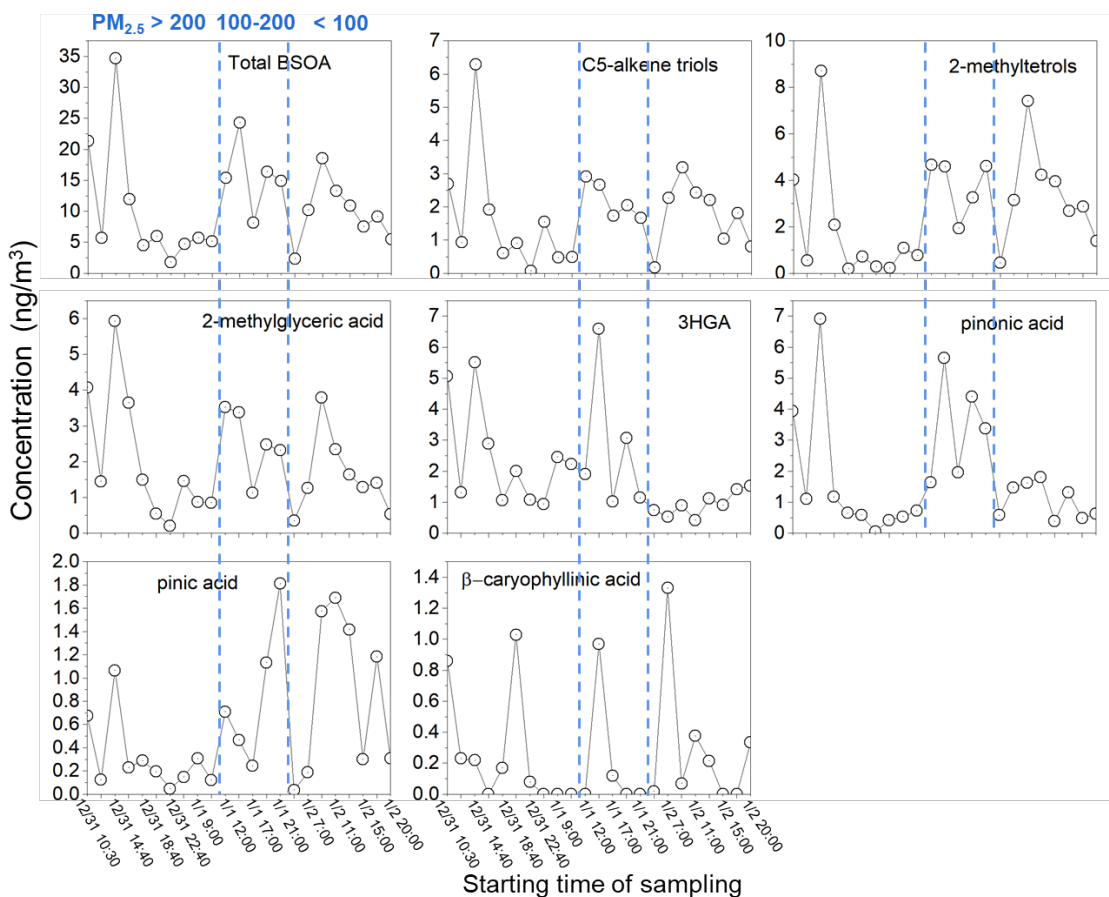
314

315

316

317

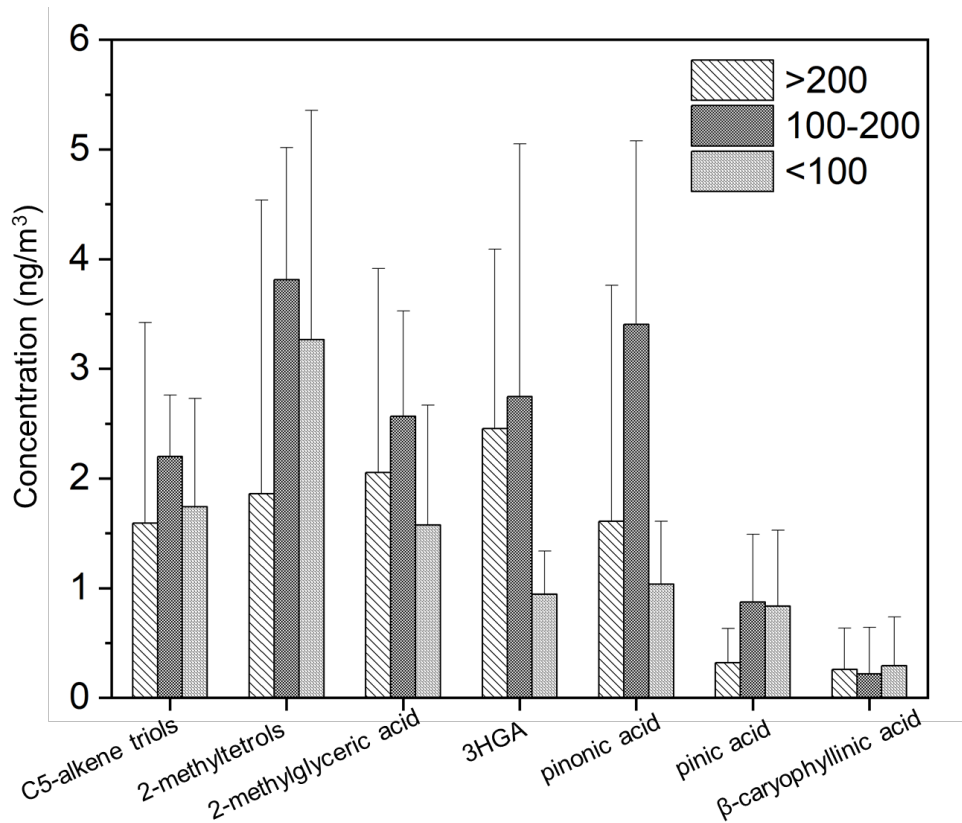
318



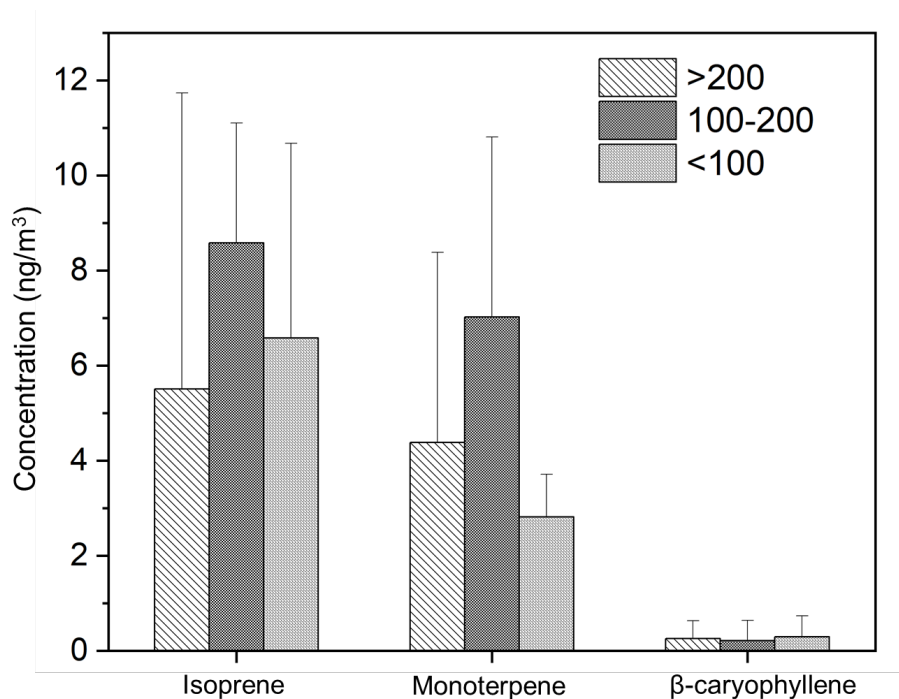
319

319 **Figure S11.** Temporal variations of ratios of biogenic SOA tracers in PM_{2.5}.

320



321
 322 **Figure S12.** Average concentrations of biogenic SOA tracers detected in three episodes
 323 according to $\text{PM}_{2.5}$ concentration (i.e., > 200, 100-200, and < 100 $\mu\text{g}/\text{m}^3$).
 324



325
 326
 327
 328
 329
 330
 331
 332
 333
 334
 335
 336
 337
 338
 339
 340
 341
 342 **Figure S13.** Average concentrations of isoprene, monoterpene, and β -caryophyllene
 343 SOA tracers detected in three episodes according to $\text{PM}_{2.5}$ concentration (i.e., > 200,
 344 100-200, and < 100 $\mu\text{g}/\text{m}^3$).
 345

346
 347
 348
 349
 350
 351
 352
 353
 354
 355
 356
 357
 358
 359
 360
 361
 362
 363
 364
 365
 366
 367
 368
 369
 370
 371
 372
 373
 374

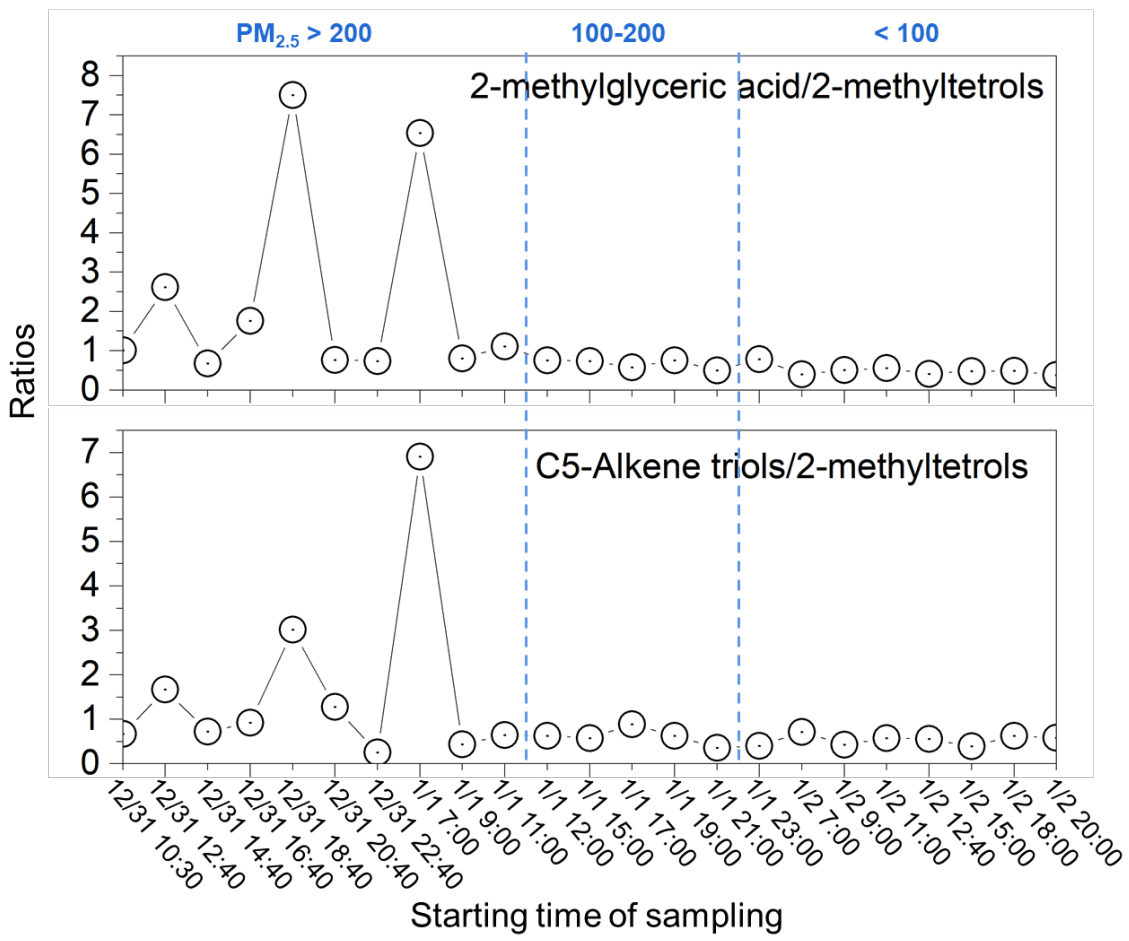


Figure S14. Temporal variations in the concentration ratios of isoprene oxidation products in $PM_{2.5}$.

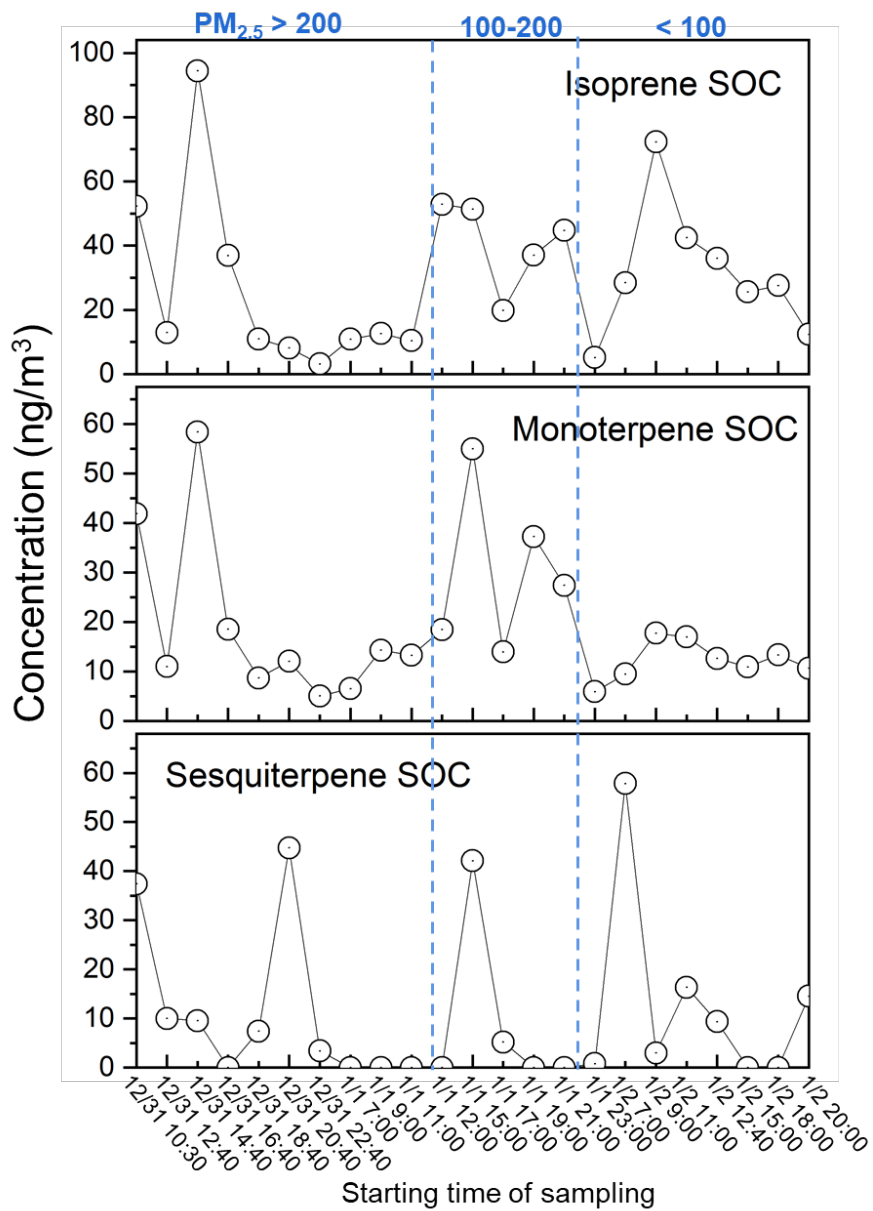


Figure S15. Temporal variations in the biogenic secondary organic carbon (SOC) derived from isoprene, monoterpene, and sesquiterpene in PM_{2.5}.

408
409
410
411
412
413
414
415
416
417
418
419
420
421
422
423
424
425
426
427
428
429
430
431
432
433
434
435
436
437
438
439
440
441
442
443

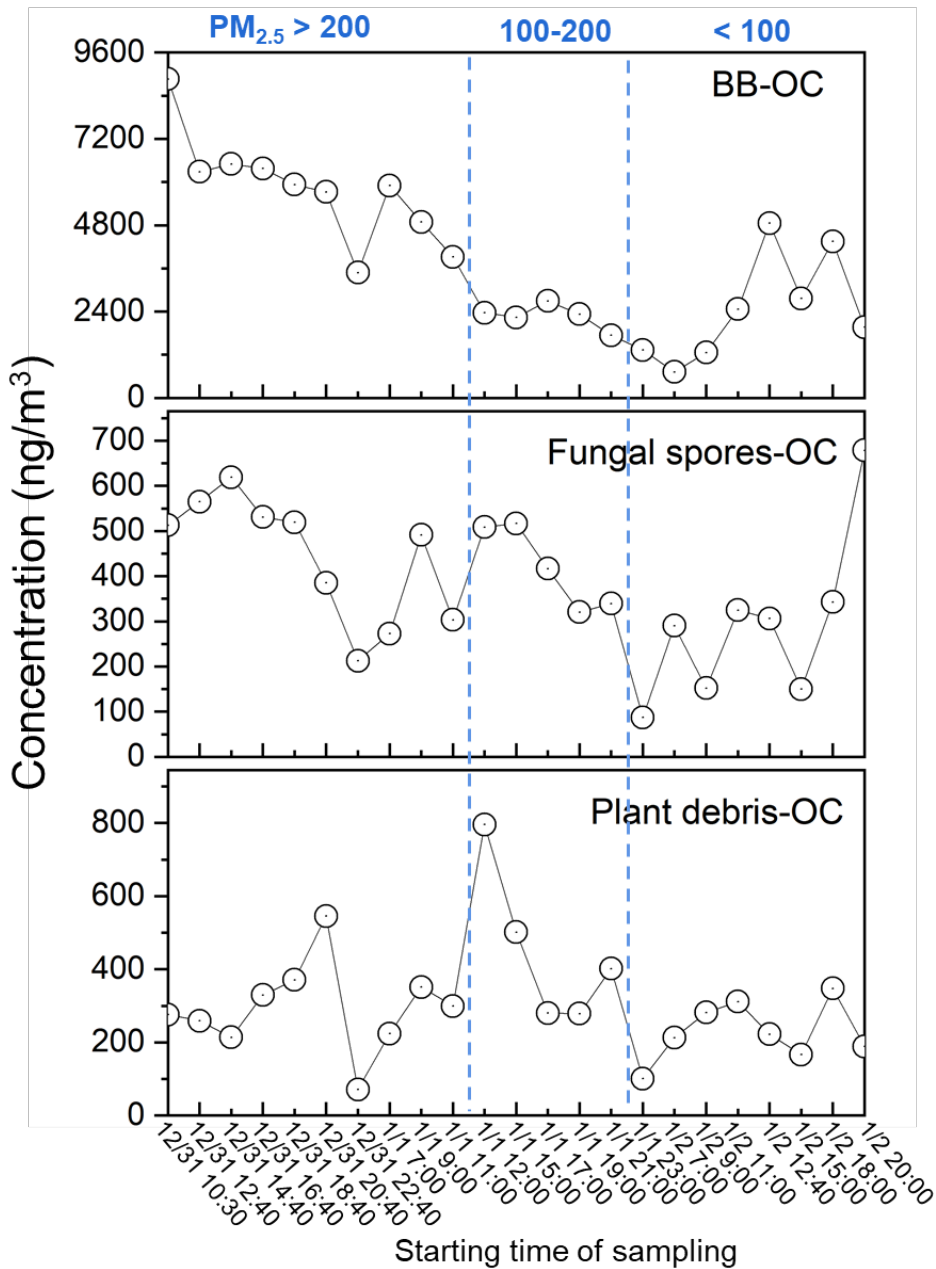


Figure S16. Temporal variations in biomass burning derived OC, fungal spores derived OC, and plant debris derived OC in PM_{2.5}.

444 **References**

445

446 Chen, L., Wang, J., Gao, Y., Xu, G., Yang, X., Lin, Q., and Zhang, Y.: Latitudinal
447 distributions of atmospheric MSA and MSA/nss-SO₄²⁻ ratios in summer over the
448 high latitude regions of the Southern and Northern Hemispheres, *Journal of*
449 *Geophysical Research: Atmospheres*, 117, <https://doi.org/10.1029/2011JD016559>,
450 2012.

451 Cheng, Y., Engling, G., He, K.-B., Duan, F.-K., Ma, Y.-L., Du, Z.-Y., Liu, J.-M., Zheng,
452 M., and Weber, R. J.: Biomass burning contribution to Beijing aerosol,
453 *Atmospheric Chemistry and Physics*, 13, 7765–7781, [https://doi.org/10.5194/acp-](https://doi.org/10.5194/acp-13-7765-2013)
454 [13-7765-2013](https://doi.org/10.5194/acp-13-7765-2013), 2013.

455 Engling, G., Carrico, C. M., Kreidenweis, S. M., Collett, J. L., Day, D. E., Malm, W.
456 C., Lincoln, E., Min Hao, W., Iinuma, Y., and Herrmann, H.: Determination of
457 levoglucosan in biomass combustion aerosol by high-performance anion-exchange
458 chromatography with pulsed amperometric detection, *Atmospheric Environment*,
459 40, 299–311, <https://doi.org/10.1016/j.atmosenv.2005.12.069>, 2006.

460 Fu, P., Kawamura, K., Okuzawa, K., Aggarwal, S. G., Wang, G., Kanaya, Y., and Wang,
461 Z.: Organic molecular compositions and temporal variations of summertime
462 mountain aerosols over Mt. Tai, North China Plain, *Journal of Geophysical*
463 *Research: Atmospheres*, 113, <https://doi.org/10.1029/2008JD009900>, 2008.

464 Fu, X., Wang, T., Wang, S., Zhang, L., Cai, S., Xing, J., and Hao, J.: Anthropogenic
465 Emissions of Hydrogen Chloride and Fine Particulate Chloride in China, *Environ.*
466 *Sci. Technol.*, 52, 1644–1654, <https://doi.org/10.1021/acs.est.7b05030>, 2018.

467 Kampf, C. J., Corrigan, A. L., Johnson, A. M., Song, W., Keronen, P., Königstedt, R.,
468 Williams, J., Russell, L. M., Petäjä, T., Fischer, H., and Hoffmann, T.: First
469 measurements of reactive α -dicarbonyl concentrations on PM_{2.5} aerosol over the
470 Boreal forest in Finland during HUMPPA-COPEC 2010 – source
471 apportionment and links to aerosol aging, *Atmospheric Chemistry and Physics*, 12,
472 6145–6155, <https://doi.org/10.5194/acp-12-6145-2012>, 2012.

473 Kawamura, K. and Ikushima, K.: Seasonal changes in the distribution of dicarboxylic
474 acids in the urban atmosphere, *Environ. Sci. Technol.*, 27, 2227–2235,
475 <https://doi.org/10.1021/es00047a033>, 1993.

476 Khare, P., Kumar, N., Kumari, K. M., and Srivastava, S. S.: Atmospheric formic and
477 acetic acids: An overview, *Reviews of Geophysics*, 37, 227–248,
478 <https://doi.org/10.1029/1998RG900005>, 1999.

479 Legrand, M. and Pasteur, E. C.: Methane sulfonic acid to non-sea-salt sulfate ratio in
480 coastal Antarctic aerosol and surface snow, *Journal of Geophysical Research:*
481 *Atmospheres*, 103, 10991–11006, <https://doi.org/10.1029/98JD00929>, 1998.

482 Li, G., Lei, W., Bei, N., and Molina, L. T.: Contribution of garbage burning to chloride
483 and PM_{2.5} in Mexico City, *Atmospheric Chemistry and Physics*, 12, 8751–8761,
484 <https://doi.org/10.5194/acp-12-8751-2012>, 2012.

485 Meng, J., Wang, G., Hou, Z., Liu, X., Wei, B., Wu, C., Cao, C., Wang, J., Li, J., Cao, J.,
486 Zhang, E., Dong, J., Liu, J., Ge, S., and Xie, Y.: Molecular distribution and stable
487 carbon isotopic compositions of dicarboxylic acids and related SOA from biogenic

488 sources in the summertime atmosphere of Mt. Tai in the North China Plain,
489 Atmospheric Chemistry and Physics, 18, 15069–15086,
490 <https://doi.org/10.5194/acp-18-15069-2018>, 2018.

491 Oros, D. R., Abas, M. R. bin, Omar, N. Y. M. J., Rahman, N. A., and Simoneit, B. R. T.:
492 Identification and emission factors of molecular tracers in organic aerosols from
493 biomass burning: Part 3. Grasses, Applied Geochemistry, 21, 919–940,
494 <https://doi.org/10.1016/j.apgeochem.2006.01.008>, 2006.

495 Paulot, F., Wunch, D., Crounse, J. D., Toon, G. C., Millet, D. B., DeCarlo, P. F.,
496 Vigouroux, C., Deutscher, N. M., González Abad, G., Notholt, J., Warneke, T.,
497 Hannigan, J. W., Warneke, C., de Gouw, J. A., Dunlea, E. J., De Mazière, M.,
498 Griffith, D. W. T., Bernath, P., Jimenez, J. L., and Wennberg, P. O.: Importance of
499 secondary sources in the atmospheric budgets of formic and acetic acids,
500 Atmospheric Chemistry and Physics, 11, 1989–2013, <https://doi.org/10.5194/acp-11-1989-2011>, 2011.

502 Sang, X., Zhang, Z., Chan, C., and Engling, G.: Source categories and contribution of
503 biomass smoke to organic aerosol over the southeastern Tibetan Plateau,
504 Atmospheric Environment, 78, 113–123,
505 <https://doi.org/10.1016/j.atmosenv.2012.12.012>, 2013.

506 Schmidl, C., Marr, I. L., Caseiro, A., Kotianová, P., Berner, A., Bauer, H., Kasper-Giebl,
507 A., and Puxbaum, H.: Chemical characterisation of fine particle emissions from
508 wood stove combustion of common woods growing in mid-European Alpine
509 regions, Atmospheric Environment, 42, 126–141,
510 <https://doi.org/10.1016/j.atmosenv.2007.09.028>, 2008.

511 Sheesley, R. J., Schauer, J. J., Chowdhury, Z., Cass, G. R., and Simoneit, B. R. T.:
512 Characterization of organic aerosols emitted from the combustion of biomass
513 indigenous to South Asia, Journal of Geophysical Research: Atmospheres, 108,
514 <https://doi.org/10.1029/2002JD002981>, 2003.

515 Stavrakou, T., Müller, J.-F., Peeters, J., Razavi, A., Clarisse, L., Clerbaux, C., Coheur,
516 P.-F., Hurtmans, D., De Mazière, M., Vigouroux, C., Deutscher, N. M., Griffith, D.
517 W. T., Jones, N., and Paton-Walsh, C.: Satellite evidence for a large source of
518 formic acid from boreal and tropical forests, Nature Geosci, 5, 26–30,
519 <https://doi.org/10.1038/ngeo1354>, 2012.

520 Wang, X., Jacob, D. J., Eastham, S. D., Sulprizio, M. P., Zhu, L., Chen, Q., Alexander,
521 B., Sherwen, T., Evans, M. J., Lee, B. H., Haskins, J. D., Lopez-Hilfiker, F. D.,
522 Thornton, J. A., Huey, G. L., and Liao, H.: The role of chlorine in global
523 tropospheric chemistry, Atmospheric Chemistry and Physics, 19, 3981–4003,
524 <https://doi.org/10.5194/acp-19-3981-2019>, 2019.

525 Wang, X., Jacob, D. J., Fu, X., Wang, T., Breton, M. L., Hallquist, M., Liu, Z., McDuffie,
526 E. E., and Liao, H.: Effects of Anthropogenic Chlorine on PM_{2.5} and Ozone Air
527 Quality in China, Environ. Sci. Technol., 54, 9908–9916,
528 <https://doi.org/10.1021/acs.est.0c02296>, 2020.

529 Wang, X., Bi, X., Li, H., Zhang, W., Dai, Q., Song, L., Li, L., Wu, J., Zhang, Y., and
530 Feng, Y.: The role of sources and meteorology in driving PM_{2.5}-bound chlorine,
531 Journal of Hazardous Materials, 441, 129910,

532 <https://doi.org/10.1016/j.jhazmat.2022.129910>, 2023.

533 Wang, Y., Zhuang, G., Tang, A., Yuan, H., Sun, Y., Chen, S., and Zheng, A.: The ion
534 chemistry and the source of PM_{2.5} aerosol in Beijing, *Atmospheric Environment*,
535 39, 3771–3784, <https://doi.org/10.1016/j.atmosenv.2005.03.013>, 2005.

536 Wang, Y., Zhuang, G., Zhang, X., Huang, K., Xu, C., Tang, A., Chen, J., and An, Z.:
537 The ion chemistry, seasonal cycle, and sources of PM_{2.5} and TSP aerosol in
538 Shanghai, *Atmospheric Environment*, 40, 2935–2952,
539 <https://doi.org/10.1016/j.atmosenv.2005.12.051>, 2006.

540 Wang, Y., Zhuang, G., Chen, S., An, Z., and Zheng, A.: Characteristics and sources of
541 formic, acetic and oxalic acids in PM_{2.5} and PM₁₀ aerosols in Beijing, China,
542 *Atmospheric Research*, 84, 169–181,
543 <https://doi.org/10.1016/j.atmosres.2006.07.001>, 2007.

544 Yang, X., Wang, T., Xia, M., Gao, X., Li, Q., Zhang, N., Gao, Y., Lee, S., Wang, X.,
545 Xue, L., Yang, L., and Wang, W.: Abundance and origin of fine particulate chloride
546 in continental China, *Science of The Total Environment*, 624, 1041–1051,
547 <https://doi.org/10.1016/j.scitotenv.2017.12.205>, 2018.

548 Ye, B., Ji, X., Yang, H., Yao, X., Chan, C. K., Cadle, S. H., Chan, T., and Mulawa, P.
549 A.: Concentration and chemical composition of PM_{2.5} in Shanghai for a 1-year
550 period, *Atmospheric Environment*, 37, 499–510, [https://doi.org/10.1016/S1352-2310\(02\)00918-4](https://doi.org/10.1016/S1352-2310(02)00918-4), 2003.

552 Yi, X., Sarwar, G., Bian, J., Huang, L., Li, Q., Jiang, S., Liu, H., Wang, Y., Chen, H.,
553 Wang, T., Chen, J., Saiz-Lopez, A., Wong, D. C., and Li, L.: Significant Impact of
554 Reactive Chlorine on Complex Air Pollution Over the Yangtze River Delta Region,
555 China, *Journal of Geophysical Research: Atmospheres*, 128, e2023JD038898,
556 <https://doi.org/10.1029/2023JD038898>, 2023.

557 Yuan, H., Wang, Y., and Zhuang, G.: MSA in Beijing aerosol, *Chin. Sci. Bull.*, 49,
558 1020–1025, <https://doi.org/10.1007/BF03184031>, 2004.

559 Zhao, W., Kawamura, K., Yue, S., Wei, L., Ren, H., Yan, Y., Kang, M., Li, L., Ren, L.,
560 Lai, S., Li, J., Sun, Y., Wang, Z., and Fu, P.: Molecular distribution and compound-
561 specific stable carbon isotopic composition of dicarboxylic acids, oxocarboxylic
562 acids and α -dicarbonyls in PM_{2.5} from Beijing, China, *Atmospheric Chemistry and
563 Physics*, 18, 2749–2767, <https://doi.org/10.5194/acp-18-2749-2018>, 2018.

564 Zhu, C., Kawamura, K., and Kunwar, B.: Effect of biomass burning over the western
565 North Pacific Rim: wintertime maxima of anhydrosugars in ambient aerosols from
566 Okinawa, *Atmospheric Chemistry and Physics*, 15, 1959–1973,
567 <https://doi.org/10.5194/acp-15-1959-2015>, 2015.

568